Rhodium complex [RhLI2]I: a novel anticancer agent inducing tumor inhibition and apoptosis

Author

Hossain, M Matakabbir, Soha, Kazi, Rahman, Arifur, Auwal, Abdul, Pronoy, Tasfik Ul Haque, Rashel, KM, Nurujjaman, M, Rahman, Habibur, Roy, Tapashi G, Khanam, Jahan Ara, Islam, Farhadul

Published

2024

Journal Title

Discover Oncology

Version

Version of Record (VoR)

DOI

10.1007/s12672-024-01632-7

Discover Oncology

Research

Rhodium complex [$RhLI_2$]I: a novel anticancer agent inducing tumor inhibition and apoptosis

M. Matakabbir Hossain[1] · Kazi Soha[1] · Arifur Rahman[1] · Abdul Auwal[1] · Tasfik Ul Haque Pronoy[1] · K. M. Rashel[1] · M. Nurujjaman[1] · Habibur Rahman[2] · Tapashi G. Roy[3] · Jahan Ara Khanam[1] · Farhadul Islam[1,4]

Received: 30 September 2024 / Accepted: 25 November 2024
Published online: 18 December 2024

Abstract
Numerous chemotherapeutic agents are currently employed in cancer treatment, but many are associated with significant side effects. This study aims to identify a novel anticancer drug that minimizes or eliminates these adverse effects. The anticancer activity of the Rhodium (III) complex cis-[$RhLI_2$]I was evaluated through both in vivo and in vitro functional assays. Apoptosis in cancer cells post-treatment was assessed using microscopy and gene expression analysis. In cytotoxicity screening via the brine shrimp lethality bioassay, the compound exhibited an LC_{50} value of 25.90 µg/mL ($P < 0.001$). It also achieved an 88.96% inhibition of cell growth ($P < 0.001$), an 82.39% increase in lifespan ($P < 0.001$), and a significant reduction in tumor weight at a dosage of 200 µg/kg in Ehrlich ascites carcinoma (EAC)-bearing Swiss albino mice. Restoration of hematological parameters, such as RBC, WBC, and hemoglobin levels, was observed in treated tumor-bearing mice compared to untreated EAC-bearing mice. The compound inhibited the growth and proliferation of breast cancer (MCF7) cells in a dose-dependent manner, achieving a maximum inhibition of 88.9% at 200 µg/mL. Apoptotic induction in MCF7 cells occurred through the upregulation of *p53, Bax, caspase-3, -8*, and *-9*, alongside the downregulation of the anti-apoptotic protein Bcl-2. No long-term adverse effects on hematological or biochemical parameters or tissue levels were observed in the mice. Given these findings, this compound demonstrates significant cytotoxic effects and has the potential to serve as a promising chemotherapeutic agent, warranting further investigation at more advanced stages.

Keywords Antineoplastic activity · Chemotherapy · Cytotoxic activity · Apoptosis · EAC cells

1 Introduction

Cancer, the second leading cause of death worldwide, poses a lifetime risk to one in five individuals and results in mortality for approximately 1 in 9 men and 1 in 12 women globally [1, 2]. More than 19 million new cases and 609,820 fatalities were reported in 2023, indicating a concerning rising trend in incidence and death rates [3]. This represents a huge increase of almost 5 million illnesses and 2 million deaths compared to the numbers reported in 2012 [4, 5]. These figures are anticipated to rise even further, with projections indicating approximately 23.6 million new cases by 2030 [5]. Thus, there is a great demand for the development of novel anticancer drugs to combat the increasing morbidity and high mortality of cancer.

✉ Farhadul Islam, f.islam@griffith.edu.au; farhad_bio83@ru.ac.bd; Jahan Ara Khanam, jakbiochem@ru.ac.bd | [1]Department of Biochemistry and Molecular Biology, University of Rajshahi, Rajshahi 6205, Bangladesh. [2]Department of Chemistry, University of Rajshahi, Rajshahi 6205, Bangladesh. [3]Department of Chemistry, Faculty of Science, University of Chittagong, Chattogram 4331, Bangladesh. [4]School of Medicine and Dentistry, Griffith University, Gold Coast Campus, Queenslan 4222, Australia.

Cancer treatment options vary widely depending on the type and stage of the disease, encompassing approaches such as surgery, radiotherapy, chemotherapy, palliative care, targeted therapies, and hormone therapy. Each modality is selected based on its suitability for the cancer's progression and specific biological characteristics. Chemotherapy, unlike surgery or radiation therapy, possesses the unique capability to eliminate cancer cells at locations distant from the primary tumor. This is achieved as chemotherapeutic agents circulate through the bloodstream, reaching and targeting metastatic sites throughout the body. Consequently, chemotherapy is classified as a systemic treatment, addressing both localized and disseminated disease [6]. Transition metal complexes, including platinum, ruthenium, rhenium, iridium, rhodium, osmium, gold, and iron, which possess anticancer properties, are currently attracting considerable attention due to their wide and diverse structural types and varied ligand bonding modes, offering significant potential for fine-tuning their biological properties [7, 8]. Accordingly, several leading chemotherapeutic agents, including cisplatin, carboplatin, and oxaliplatin, are metal-based complexes that exert their cytotoxic effects by forming irreversible coordination bonds with DNA and inhibit the DNA replication [9]. Platinum-based chemotherapeutics are used in around 10–20% of cancer patients' treatment regimens due to their excellent therapeutic efficacy [9]. Cisplatin and its structural analogues have been extensively employed in the therapeutic management of a broad spectrum of malignancies, including ovarian, bladder, cervical, testicular, and lung carcinomas, as well as hematologic cancers such as lymphomas and myelomas, and even aggressive skin cancers like melanomas [10].

Despite the development of numerous chemotherapeutic agents, many fail to achieve optimal therapeutic efficacy. This is largely due to their toxicity toward healthy, rapidly dividing cells, lack of target selectivity, suboptimal potency, and the emergence of drug resistance. Drug resistance is an adverse condition where a drug loses its efficacy in treating a disease condition driven by a number of factors, including P-glycoprotein (P-gp), non-coding RNAs, and macro-autophagy [11]. Also, hyperactivity of drug transporters plays a pivotal role in fostering drug resistance by diminishing the accumulation of chemotherapeutic agents at tumor sites. Key players in this mechanism include P-glycoprotein (P-gp), SOX9, and GRP78, which enhance the activity of drug efflux transporters, thereby mediating chemoresistance [12]. Furthermore, the induction of pro-survival autophagy, driven by endoplasmic reticulum (ER) stress-associated proteins such as IRE1, ATF4, and PERK, is implicated in promoting drug resistance [12]. The overexpression of long non-coding RNA HULC in breast cancer further exemplifies this adaptive response by activating the PI3K-AKT/PKB signaling pathway through IGF1R, thereby inducing cisplatin resistance and augmenting tumor invasiveness [13]. Consequently, these limitations often lead to adverse effects, including gastrointestinal toxicity, nephrotoxicity, and common symptoms such as nausea and vomiting, which further complicate treatment regimens [9, 14, 15]. To address these drawbacks, research efforts have increasingly focused on the development of novel metal-based therapeutics with enhanced selectivity for tumor cells, aiming to minimize adverse effects [15].

Rhodium complexes have garnered significant interest due to their highly tunable reactivity, ranging from kinetically labile to substitutionally inert species, coupled with their excellent water solubility and relative accessibility with a wide range of biological applications [10, 15]. For example, Rh (III) complexes can bind to biomolecules and are also employed for cell imaging and small molecule sensors [10]. Moreover, several rhodium complexes have recently been described as highly effective antiproliferative agents against several human cancer cells, making them possible alternatives to Pt- and Ru-based metallodrugs [16-17]. Rh (III) complexes, for instance, boost the expression of tumor suppressor genes [18]. Also, Rh(III) complexes can stop the growth of cancer cells by blocking the signal transducer and activator of transcription 3 (STAT3) signaling pathway [19]. In addition, Rh(III) complexes have also been shown to inhibit kinase activity and bind specifically to thermodynamically destabilized DNA mismatch sites through a binding mode known as metalloinsertion [9, 10].

Moreover, the biological activity of metal complexes can be increased by combination with cytotoxic ligands and targeting multiple cellular mechanisms [20]. Ligand substitution can further improve the cytotoxicity of rhodium complexes. For example, 5,6-dimethyl substituted ligand of phenanthroline demonstrated 18-times higher anticancer activity than the non-substituted phenanthroline [21]. Additionally, studies have reported that mer-[RhCl3(NH3)3] had strong antiproliferative effects and prolonged the lifespan of mice with ascetic sarcoma [22]. In vitro cytotoxicity assessments revealed that Rh(III) complex incorporating a camphor-derived ligand with four methyl substituents exhibits greater efficacy and cytotoxicity against the HCT-116 cancer cells compared to complexes with three methyl groups or those with terpyridine ligands [23]. The coordination of biologically active ligands with a transition metal core can yield complexes with distinct biological and physicochemical characteristics [24]. Consequently, the judicious selection of ligands is essential for optimizing the cytotoxic properties of these complexes [21]. Therefore, herein, we have examined the cytotoxic and antineoplastic properties of a newly synthesized rhodium complex $[RhLI_2]I$ (ligand L is a 14-membered octamethyl

tetraazamacrocycle, Me_8 [14] diene), evaluating its efficacy against the MCF7 cells and Ehrlich ascites carcinoma (EAC) cells to identify a potential chemotherapeutic agent.

2 Materials and methods

2.1 Chemicals and reagents

All the chemicals and reagents used in the experiment were analytical grade and purchased from Thermo Fisher Scientific Inc. Waltham, MA USA, Promega, Madison, Wisconsin, USA, Amresco, 11 Speen Street Framingham, Massachusetts, USA, Life Technologies, 5791 Van Allen Way Carlsbad, CA, USA, Applied Biosystems, 180 Oyster Point Blvd South San Francisco, CA, USA.

2.2 Synthesis and characterization of rhodium (III) complex *cis*-[$RhLI_2$]I

3,10-C-meso-3,5,7,7,10,12,14,14-octamethyl-1,4,8,11-tetraazacyclotetradeca-4,11-diene. $2HClO_4$ (3,10-C-meso-Me_8 [14] diene. $2HClO_4$) ligand was synthesized by established protocol and isolated the 3,10-C-meso-3,5,7,7,10,12,14,14-octamethyl-1,4,8,11-tetraazacyclotetradeca-4,11-diene which was used as a free ligand (L) bind with the Rhodium complex [25, 26]. Rhodium (III) complex *cis*-[$RhLI_2$]I was synthesized in three steps; synthesis of free ligand 3,10-C-meso-Me_8 [14] diene (L), formation of Rhodium (III) complex *cis*-[$RhLCl_2$]Cl and preparation of Rhodium (III) complex *cis*-[$RhLI_2$]I as previously reported [26].The compound was characterized using its physical properties, infrared (IR), electronic spectral and magnetochemical data and ^{1}H-NMR spectral data [26].

2.3 Animals and cancer cell lines

Approval for the use of experimental animal (mouse) was obtained from the University ethic committee (Institutional Animal, Medical Ethics, Bio-Safety and Bio-Security Committee for Experimentations on Animal, Human, Microbes, and Living Natural Sources (No. 293(13)/320-IAMEBBC/IBSc), Institute of Biological Sciences, Rajshahi University, Bangladesh. Adult male Swiss albino mice weighing between 20 and 23 g were used. These mice were reared in our laboratory and meticulously adhered to the standards and regulations imposed by the Institutional Animal, Medical Ethics, Bio-Safety and Bio-Security Committee.

Ehrlich Ascites Carcinoma (EAC) cells were collected from the Indian Institute for Chemical Biology (IICB) in Kolkata, India, with their gracious cooperation. These cells were kept alive by administering 10^5 cells per animal intraperitoneally every two weeks in a controlled ambient condition in our departmental laboratory**.** While, breast cancer (MCF7) cells were recruited from the American type of cell culture (ATCC) and was maintained in Dulbecco's Modified Eagle Medium (DMEM) with the supplementation of 10% fetal bovine serum (FBS) and 1% penicillin/ streptomycin at 37 ℃ in presence of 5% CO_2.

2.4 Brine shrimp lethality bioassay

The cytotoxic effect of Rhodium (III) complex, *cis*-[$RhLI_2$]I was evaluated using an in vivo assay against Brine shrimp nauplii following the established protocol [27]. The assay involved exposing nauplii to six different concentrations of the complex (2, 4, 6, 8, 10, and 15 µg/mL) in 5 mL of simulated seawater for a 24 h period. Mortality rates were subsequently recorded and analyzed to determine the median lethal concentration (LC_{50}) via regression analysis.

2.5 Inhibition of EAC cell growth

Tumor cell growth inhibition in vivo was evaluated following a standardized protocol [28]. Herein, three groups of mice with each group comprising six mice. On the first day, each mouse was inoculated with 1.6×10^6 EAC cells. Treatment commenced 24 h post-inoculation and continued for five consecutive days. Groups 2 and 3 received the rhodium (III) complex intraperitoneally at dosages of 100 mg/kg and 200 mg/kg body weight, respectively, with each mouse receiving a daily injection volume of 0.1 ml. Group 1, serving as the control, was administered normal saline intraperitoneally. On the sixth day, the mice were sacrificed, and peritoneal fluid was harvested using 0.9% saline. The viable tumor cells

were quantified using a hemocytometer following trypan blue staining, and tumor cell growth inhibition was calculated using the prescribed formula.

$$\% \text{ Cell growth inhibition } = (C - T / C) \times 100$$

where, T = Mean of tumor cells in the treated group of mice and C = Mean of tumor cells in the control group of mice.

2.6 Average tumor weight and survival time

Survival time and tumor weight were evaluated using the method described previously [29]. The experiment included three groups of mice, with six mice per group, each receiving an inoculation of 1.6×10^6 EAC cells on the first day. The control group (Group 1) was administered normal saline. Treatment with the test compound was initiated intraperitoneally 24 h post-inoculation for Groups 2 and 3, at doses of 100 mg/kg and 200 mg/kg body weight, respectively, and continued for a duration of 10 days. The body weight of each mouse was recorded at 48 h intervals, with monitoring extending up to 25 days from the initial day of inoculation. Survival time was documented and expressed as mean survival time (MST) in days, with the percentage increase in life span (% ILS) calculated according to the prescribed formula:

$$\text{MST } = (\Sigma \text{ Survival time in days of each mouse in a group})/\text{Total number of mice}$$

$$\% \text{ ILS } = (\text{MST of treated group / MST of control group} - 1) \times 100$$

2.7 Hematological profile

The hematological parameters, specifically WBC, RBC, and hemoglobin (Hb), were assessed using cell dilution fluids and a hemocytometer to evaluate the impact of the rhodium (III) complex on the hematological profile of EAC cell-bearing mice [30]. All groups were intraperitoneally injected with 0.1 mL of 1.6×10^6 EAC cells per mouse on day zero. Following a 24 h inoculation period, Groups 3 and 4 were administered the test compound at doses of 100 mg and 200 mg per kg of body weight per day, respectively, for 10 consecutive days. Group 1 consisted of normal mice, while Group 2, designated as the control group, included EAC-bearing mice only. Each group comprised of six mice. On the 12th day of post-inoculation, blood samples were collected via tail puncture, and the hematological parameters were measured accordingly [28].

2.8 Inhibition of MCF-7 cell growth by MTT assay

The antiproliferative study of the rhodium (III) *cis*-[$RhLI_2$]I complex against MCF-7 cell in vitro was examined using MTT (3-[4,5-dimethylthiazol-2-yl]−2,5 diphenyl tetrazolium bromide) colorimetric technique according to the publish protocol [31]. In a 96-well plate, each well containing 100 µl of MCF-7 cells (5 × 10^5 cells/well) suspended in 100 µl of RPMI-1640 media, five graded concentrations of the compound (200 µg, 100 µg, 50 µg, 25 µg, and 10 µg/ per mL) were administered, with control wells excluded, followed by incubation at 37 °C in a 5% CO_2 atmosphere for 24 h. After removing the aliquots from each well, 180 µL of PBS and 20 µL of newly produced MTT were added and incubated at 37 °C for 8 h. The aliquot was removed from each well and 200 µl of acidic isopropanol was added, then the mixture was incubated for an additional hour at 37 °C. A titer plate reader was used to measure each well's absorbance at 570 nm, and the proliferation inhibition was determined using the equation below.

$$\begin{aligned} \text{Proliferation inhibition } (\%) &= \{(A - B)/A\} \times 100, \text{ Where A} \\ &= \text{Absorbance of control (withoutcompound) and B} \\ &= \text{Absorbance treatment.} \end{aligned}$$

2.9 Morphological appearance and nuclear damage

The induction of apoptosis in MCF7 cells by tested compound was assessed following a previously established protocol [32]. Morphological analysis of MCF7 cells in both the treated group (administered at 200 mg/kg body weight/day)

and the control group was performed using an Olympus IX71 fluorescence microscope (Olympus, Seoul, Korea). In brief, MCF7 cells were harvested from culture dishes containing RPMI-1064 medium, treated with the test compound and saline (none treated control disc). The cells were subsequently stained with Hoechst 33342 (0.1 µg/mL) at 37 °C for 20 min to visualize nuclear morphology. Post-staining, the cells were thoroughly washed with phosphate-buffered saline (PBS) and resuspended in PBS to facilitate the observation of apoptotic morphological changes under fluorescence microscopy. To further assess necrosis or late-stage apoptotic cell death, the MCF7 cells underwent an additional wash with 0.01% sodium azide in 0.9% NaCl. Following this, the cells were stained with propidium iodide (PI), washed again, and resuspended in PBS for detailed morphological examination under the fluorescence microscope.

2.10 mRNA extraction and cDNA synthesis

Total RNA from both treated and non-treated MCF-7 cells was isolated using RNA extraction kit (Favorgen, Taiwan) following the manufacturer's guidelines. The RNA concentration and purity were precisely quantified using the Thermo Scientific NanoDrop One, with mean absorption ratios A260/280 and A260/230 critically evaluated to confirm sample purity. The structural integrity of the RNA was further validated through 1.8% agarose gel electrophoresis. cDNA synthesis was performed using the High-Capacity cDNA Reverse Transcription Kit (Promega, Madison-Wiscosin, USA) following the manufacturer's protocol and guidelines. In brief, two micrograms of total RNA were reverse transcribed into cDNA using 1 µL Random Primer, 2 µL of 2.5 mM $MgCl_2$, 1 µL GoScript™ Reverse Transcriptase, 1 µL PCR Nucleotide Mix (final concentration of 0.5 mM each dNTP), 4 µL GoScript™ 5X Reaction Buffer, and nuclease-free water to achieve a final reaction volume of 20 µL. The synthesized cDNA was then stored at – 20 °C until subsequent analysis.

2.11 Real-time quantitative PCR (RT-qPCR)

The expression of key apoptosis-related genes, such as *p53, Bax, Parp, Caspase-3, –8, –9* and *Bcl-2*, etc., was analyzed via RT-qPCR (LightCycler 96, Roche Diagnostics, Forrenstrasse 2, 6343 Rotkreuz, Switzerland), utilizing glyceraldehyde-3-phosphate dehydrogenase (GAPDH) as a housekeeping control. The sequences of the primers utilized in the experiment are detailed in Table 1. Each 20 µL PCR reaction mixture comprised 10 µL of master mix (Promega, Madison, WI, USA), 1 µL each of forward and reverse primers, 2 µL of template (50 ng of cDNA), and 6 µL of nuclease-free water. The PCR amplification was conducted with an initial denaturation at 95 °C for 10 min, followed by 45 cycles of 15 s at 95 °C for denaturation and 1 min at 60 °C for annealing and extension. The resultant data were analyzed using the comparative Ct (ΔΔCt) method, which involves calculating the relative expression levels by comparing the

Table 1 List of primers used in the current study

Gene	Primer	Sequence (5′––––––––––––––––3′)
PARP	F	GGCCTCGGTGGATGGAATG
	R	GCAAACTAACCCGGATAGTCTCT
P53	F	GCC CAA CAA CAC CAG CTC CT
	R	CCT GGG CAT CCT TGA GTT CC
BAX	F	CCCGAGAGGTCTTTTTCCGAG
	R	CCAGCCCATGATGGTTCTGAT
BCL2	F	GGTGGGGTCATGTGTGTGG
	R	CGGTTCAGGTACTCAGTCATCC
CASPASE 3	F	CATGGAAGCGAATCAATGGACT
	R	CTGTACCAGACCGAGATGTCA
CASPASE 8	F	ACA CAG TCG AGT AGA CTC TCAAA
	R	AGG AAG TGA TGC TCG TTC AGA
CASPASE 9	F	CTG TCT ACG GCA CAG ATG GAT
	R	GGG ACT CGT CTT CAG GGG AA
GAPDH	F	GGAGCGAGATCCCTCCAAAAT
	R	GGCTGTTGTCATACTTCTCATGG

target gene quantity to that of the endogenous control GAPDH. Melting curve analysis, with a temperature gradient from 60 °C to 95 °C at 0.3 °C increments, was employed to identify the melting temperatures of specific amplification products and primer dimers.

2.12 Toxicity studies in vivo

2.12.1 Effect of test compound on biochemical and haematological parameters

Estimations of the biochemical parameters were carried out by a bioanalyzer (Humalyzer 3000, HUMAN Diagnostics Worldwide, Wiesbaden, Germany). For this study, mice (n = 40), each weighing between 19 and 21 g, were allocated into one of two distinct groups: a control group (n = 20 male mice) and a high-dose treatment group (n = 20 male mice). Moreover, the mice in the treatment group were administered the rhodium (III) complex intraperitoneally at dosages of 200 mg/kg by a 1 ml syringe over a 10 day period. After the treatment, both of the groups of mice were anesthetized using diethyl ether and sacrificed on 10 day, day 15 and day 25 with the help of a surgical blade No.22. Finally, fresh blood was withdrawn to collected in no ethylenediamine tetra-acetic acid (EDTA) coated vial from the heart by 3 ml syringe. In addition, the blood sample were allowed to clot at 40 °C for 4 h. After clotting, the blood samples were centrifuged at 4000 rpm for 15 min using a WIFUNG centrifuge LABO-50 M. Finally, the clear straw color serum was collected in vials with a Pasteur pipette and stored at − 20 °C. Biochemical parameters were analyzed as previously described [33].

Fresh blood from the animal of was withdrawn to collected in ethylenediamine tetra-acetic acid (EDTA) coated vial from the heart by 3 ml syringe. The hematological parameters, (WBC, RBC, and Hb), were assessed following a standard method [34]. In addition, effects of the compound on cellular level are examined by histopathology of major organs of animals receiving the compound followed by the protocol published previously [35].

2.13 Statistical analysis

Data (percent of cell growth inhibition, increase of life span, body/tumor weight and hematological profile) are expressed as mean ± SEM (Standard Error of Mean). Data have been analyzed with one-way analysis of variance (ANOVA) followed by Duncan's multiple range test using GraphPad Prism 8 software. Where $P < 0.05$ was considered to be statistically significant.

3 Results

3.1 The structure of the rhodium (III) complex cis-[$RhLI_2$]I

This complex can be ascribed an entirely equatorially orientated structure in Fig. 1A. Structurally deep explanation of this rhodium (III) complex cis-[$RhLI_2$]I was given a previous published article [26].

3.2 Brine shrimp lethality bioassay

The cytotoxicity of the rhodium (III) complex cis-[$RhLI_2$]I was conducted using brine shrimp lethality bioassay. The median lethal concentration (LC_{50}) was calculated to be 25.90 µg/ml. Also, the percentage mortality of nauplii increased in correlation with the concentration of the test compound, as illustrated in Fig. 1B.

3.3 Inhibition of EAC cell growth

In vivo tumor cell growth inhibition was observed with rhodium (III) complex cis-[$RhLI_2$]I at two different doses (100 µg and 200 µg/kg of body weight) per mouse per day as illustrated in Fig. 1C& D. The highest cell growth inhibition (88.96%) was found with the 200 µg/kg dosage compared with the control group ($p < 0.001$), while test compound at 100 µg/kg inhibited cell growth by 82.396% in comparison to that of untreated EAC-bearing mice.

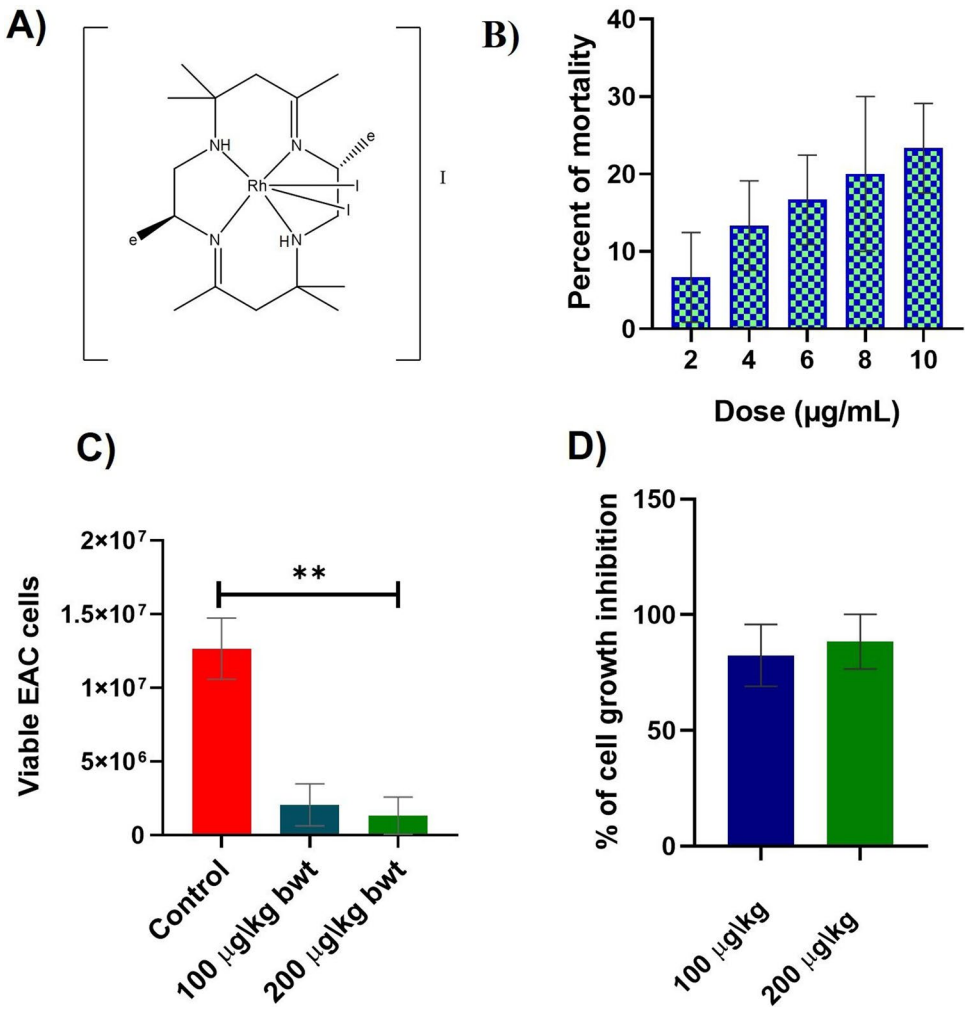

Fig. 1 In vivo cytotoxic activity of the compound. **A** Structure of the Rhodium (III) complex *cis*-[$RhLI_2$]I. **B** The compound showed cytotoxicity against brine shrimp nauplii in a dose dependent manner with an LC_{50} value of 25.90 µg/ml. **C** Number of viable EAC cells. **D** percentage of EAC cell growth inhibition. The results are presented as mean ± SEM. Significant values are indicated by **P < 0.01 and ***P < 0.001 when compared to the control group (EAC bearing only)

3.4 Average tumor weight and survival time

As illustrated in Fig. 2A, the rhodium (III) complex cis-[$RhLI_2$]I exhibits a pronounced impact on tumor proliferation. In the control group (EAC-bearing mice), a substantial increase in body weight of 63.33% was observed by day 20 in comparison to that of normal animal. In contrast, administration of the rhodium (III) complex cis-[$RhLI_2$]I at a dose of 200 µg/kg (intraperitoneally) led to a significantly attenuated weight gain of 39.16% ($p < 0.001$) over the same period. Further analysis demonstrated that this dosage elicited a marked reduction in tumor burden, with a 38.16% decrease in average tumor weight compared to the control EAC-bearing group. As illustrated in Fig. 2B, the rhodium (III) complex cis-[$RhLI_2$]I also exerted a profound effect on survival outcomes. Treatment at 200 µg/kg (i.p.) significantly extended the lifespan of tumor-bearing mice, yielding a 44.44% increase ($p < 0.001$) in survival duration relative to untreated controls.

3.5 Hematological profile

During tumor progression, deviations in hematological parameters from baseline levels were observed. Only EAC-bearing mice exhibited decreased hemoglobin levels (% of Hb) and a reduced number of red blood cells (RBC) compared to normal mice, while total white blood cell count (WBC) was elevated. Administration of the rhodium (III) complex cis-[$RhLI_2$]I at 200 µg /kg (i.p.) per day led to a moderate normalization of hematological parameters Table 2.

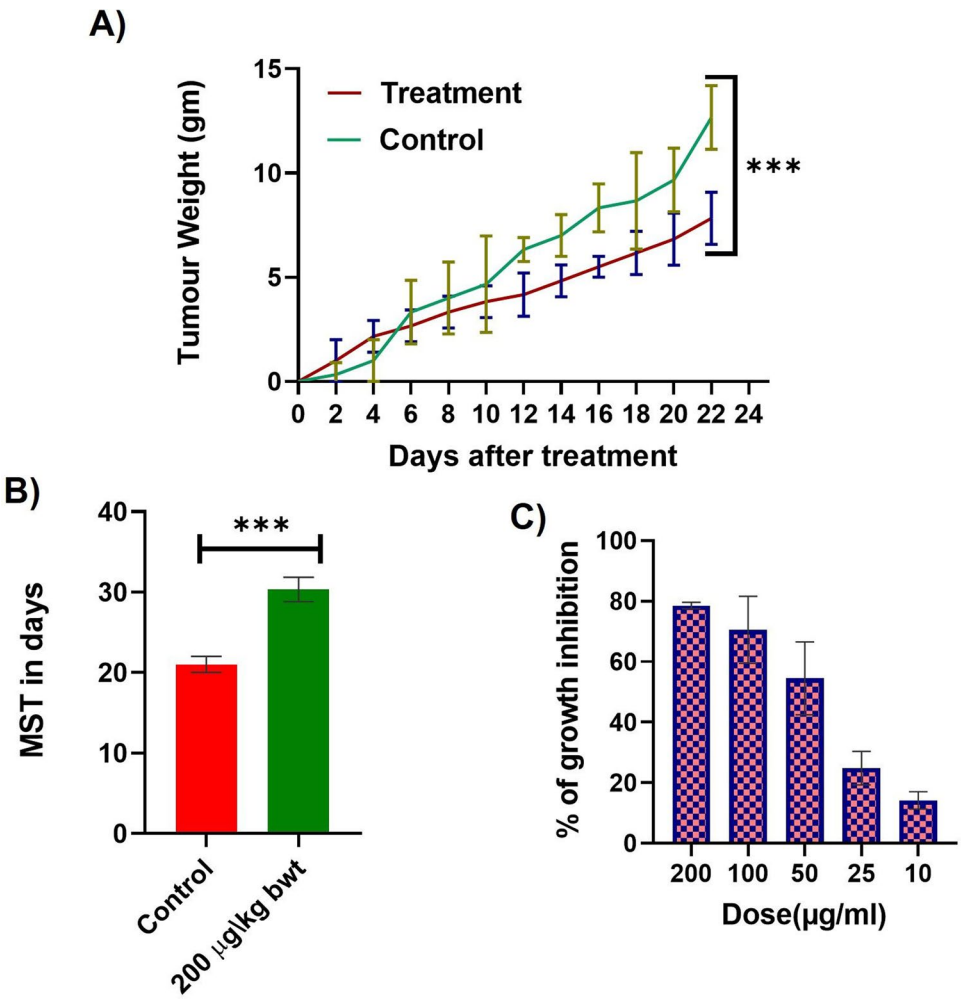

Fig. 2 Effects of tested compound on tumor weight and survival of EAC-bearing mice. **A** Effect of rhodium (III) complex *cis*-[$RhLI_2$]I on tumor weight of EAC-bearing mice. **B** Effects of rhodium (III) complex *cis*-[$RhLI_2$]I on survival time of EAC-bearing mice. **C** percentages of growth inhibition of MCF7 cells in comparison to that of untreated cells. The results are presented as mean ± SEM. Significant values are indicated by ***P < 0.001 when compared to the control group

Table 2 Effects of the rhodium (III) complex *cis*-[$RhLI_2$]I on hematological parameters in normal and experimental mice on day 12 of tumor inoculation

Name of experiment	RBC cells/mL	WBC cells/ mL	% of Hb gm/dL
Normal mice	$(1.44 \pm 0.11) \times 10^{11}$	$(0.241 \pm 0.54) \times 10^{9}$	9.033 ± 0.08
Control (EAC bearing mice)	$(1.12 \pm 0.04) \times 10^{11}$	$(2.80 \pm 0.78) \times 10^{9}$	7.33 ± 0.33
Treatment (EAC + 200 µg/kg body weight/day)	$(1.32 \pm 0.02) \times 10^{11}$*	$(2.65 \pm 0.62) \times 10^{9}$*	8.63 ± 0.317*

The results are presented as mean ± SEM. Significant values are indicated by *P < 0.05 when compared to the normal and control groups

3.6 Inhibition of MCF7 cell growth

Following 24 h of incubation, the rhodium (III) *cis*-[$RhLI_2$]I complex demonstrated a dose-dependent reduction in MCF7 cells viability as depicted in Fig. 2C. At a concentration of 200 µg/mL, the compound achieved a 78.5% inhibition of MCF7 cell growth. As the concentration was reduced to 100, 50, 25, and 10 µg/mL, the inhibition correspondingly decreased to 70.5%, 54.5%, 24.9%, and 14.1%, respectively. The IC_{50} values of test compound against MCF7 was calculated to be 81.6 µg/ml.

3.7 Morphological appearance and nuclear damage

Following 24 h exposure to the rhodium (III) *cis*-[$RhLI_2$]I complex (200 mg/mL), distinct morphological changes were observed in MCF7 cells. In the control group, MCF7 cell nuclei appeared round, regular, and uniformly stained with

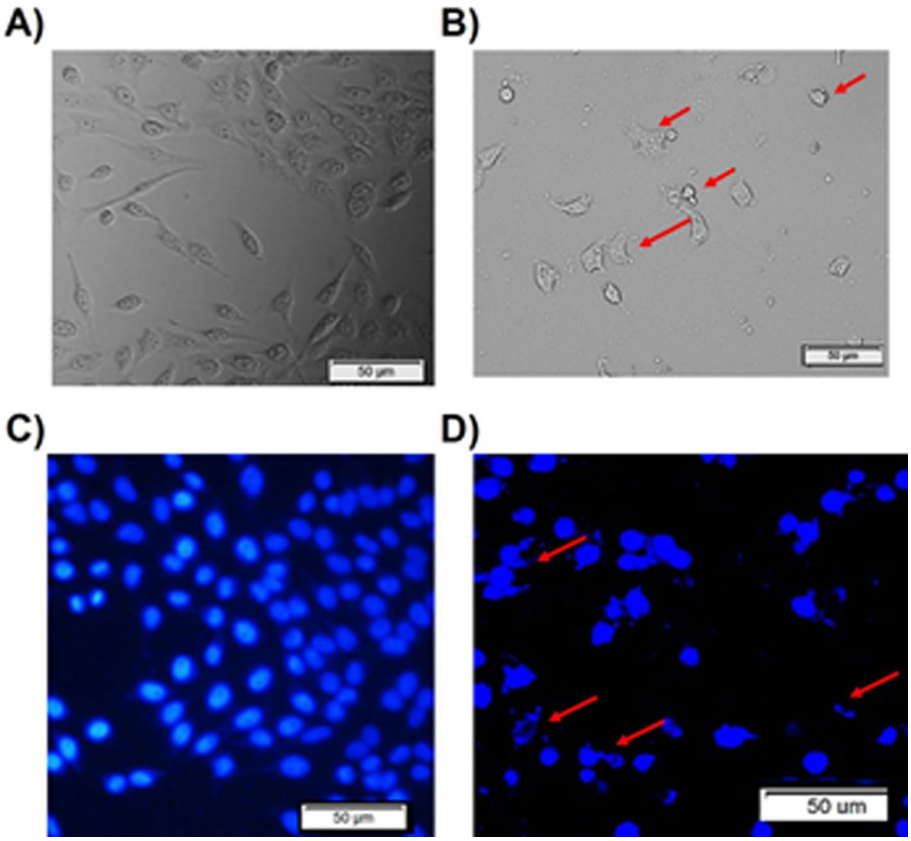

Fig. 3 Microscopic view of control and treated MCF7 cells. **A** Control MCF7 cells shown no apoptotic features under optical microscope. **B** MCF7 cells treated with the compound shown nuclear condensation, fragmentation, cell membrane blebbing, apoptotic bodies, etc., (indicated by red arrows) under optical microscope. **C** Control MCF7 cells shown no apoptotic (round and smooth nuclear material, intact membrane etc.,) features under fluorescence microscope. **D** MCF7 cells treated with the compound shown nuclear condensation, fragmentation, cell membrane blebbing, apoptotic bodies, etc., (indicated by red arrows) under fluorescence microscope

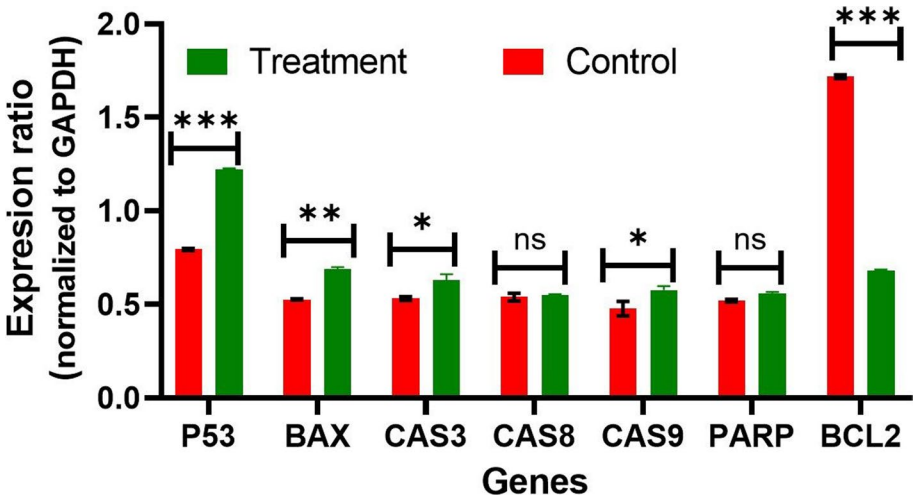

Fig. 4 Effect of test compound apoptotic gene expression. Relative expression of *p53, Bax, Bcl2, Caspas 3, Caspas 8,* and *PARP* in MCF7 cells in vitro treated and untreated with the test compound. Total RNA was extracted and reverse transcribed, and the generated DNA served as a template for a qPCR relative expression analysis with SYBR green master mix. Data were analyzed by ΔΔ CTs and normalized to (GAPDH) house-keeping gene. (The results are presented as mean ± SEM. Significant values are indicated by *P < 0.05,**P<0.01 and ***P < 0.001 when compared to the control group

Hoechst 33342 (Fig. 3). In contrast, the treated group exhibited distinct apoptotic features, including chromatin condensation, membrane blebbing, and apoptotic bodies, clearly observed via fluorescence microscopy (Fig. 3).

3.8 Gene expression analysis

We hypothesized that the rhodium (III) *cis*-[$RhLI_2$]I complex demonstrated the potential antiproliferative efficiency against MCF-7 following induction of apoptosis. Consequently, we sought to assess the expression levels of genes associated with apoptosis. We examined the effect of the test compound on the expression of pro-apoptotic genes, including *p53, Bax, Caspase 3, Caspase 8,* and *PARP*, as well as the anti-apoptotic gene *Bcl-2*, using RT-PCR. Pro-apoptotic genes, including *p53, Bax, Caspase 3, Caspase 8*, and *PARP*, were found to be overexpressed in the treated group compared to the control, as illustrated in the Fig. 4. However, the expression of the anti-apoptotic gene *Bcl-2* was lower compared to the control.

3.9 Biochemical profile of blood

After a 10-day treatment of Swiss albino mice with the rhodium (III) *cis*-[$RhLI_2$]I complex at a dose of 200 µg/kg administered intraperitoneally, significant changes were observed in key biochemical parameters, including blood glucose, serum cholesterol, creatinine, Serum Glutamic-Oxaloacetic Transaminase (SGOT), and Serum Glutamic Pyruvic Transaminase (SGPT). Blood glucose levels showed a slight decrease compared to untreated controls at day 0, while serum cholesterol levels exhibited a modest increase throughout the treatment. Renal function, assessed via creatinine levels, showed only minor differences between treated and untreated groups during the treatment period. Liver function, monitored by SGOT and SGPT, revealed a slight decrease in SGOT and a slight increase in SGPT levels during the experiment. Following the treatment period, all parameters, including blood glucose, serum cholesterol, creatinine, SGOT, and SGPT, returned to baseline levels (Fig. 5). Similarly, haematological parameters of mice receiving the tested compound for 10 consecutive days showed mild deterioration during treatment, however, the parameters restored back towards normal levels following the treatment (Table 3).

Also, the histopathological result showed that there was no damage (regeneration, degeneration etc.,) on kidney, lung, heart, and liver tissues in treated mice, indicating there is adverse effects of the tested compound on tissue levels in mice Fig. 6.

4 Discussion

A number of metal-based chemotherapeutic drugs is being using for the treatment of patients with various cancers, however, severe side effects, high cost and unavailability limit their application in clinical settings. Thus, focus of our current research is searching for alternative chemotherapeutic agents with no or minimal adverse effects on host. In this study, we reported the anticancer effect of the synthetic Rhodium complex [$RhLI_2$]I at various doses against EAC cell-induced cancer proliferation, growth and survival. Additionally, the compound induced MCF7 cells dead followed by activation of intrinsic mitochondrial pathway in a dose dependent manner. Host toxicity study revealed that the tested compound has no long-term effect on major organs at tissue levels along with no or minor effects on haematological and biochemical parameters in mice.

The cytotoxic potential of the Rhodium complex was screened using the brine shrimp lethality bioassay. A drug with an LC_{50} value of less than 250 µg/ml against brine shrimp lethality assays is a promising option for future research [29]. A moderate LC_{50} (25.9 µg/ml) value indicating the potential pharmacological potential of the tested compound. Thus, dose dependent cytotoxic effect against brine shrimp nauplii could be link to the possible anticancer activities [36]. For example, the synthetic Rhodium complex significantly slowed down tumor (EAC) growth, markedly reduced tumor weight (volume), and considerably increased the lifespan of EAC-induced mice. The regression of tumor size, weight and increase of survival time was recognized as the primary objective end-point of effectiveness in preclinical and clinical trials of a potential chemo-agent [31].

The level of hematological parameters considered as significant markers for screening of anticancer agents against EAC-induced cancer model [37]. Since, cancer can directly induce anemia through the suppression of hematopoiesis or by generating cytokines that impede RBC production [38], thus, in EAC-bearing mice RBC count could be reduce with

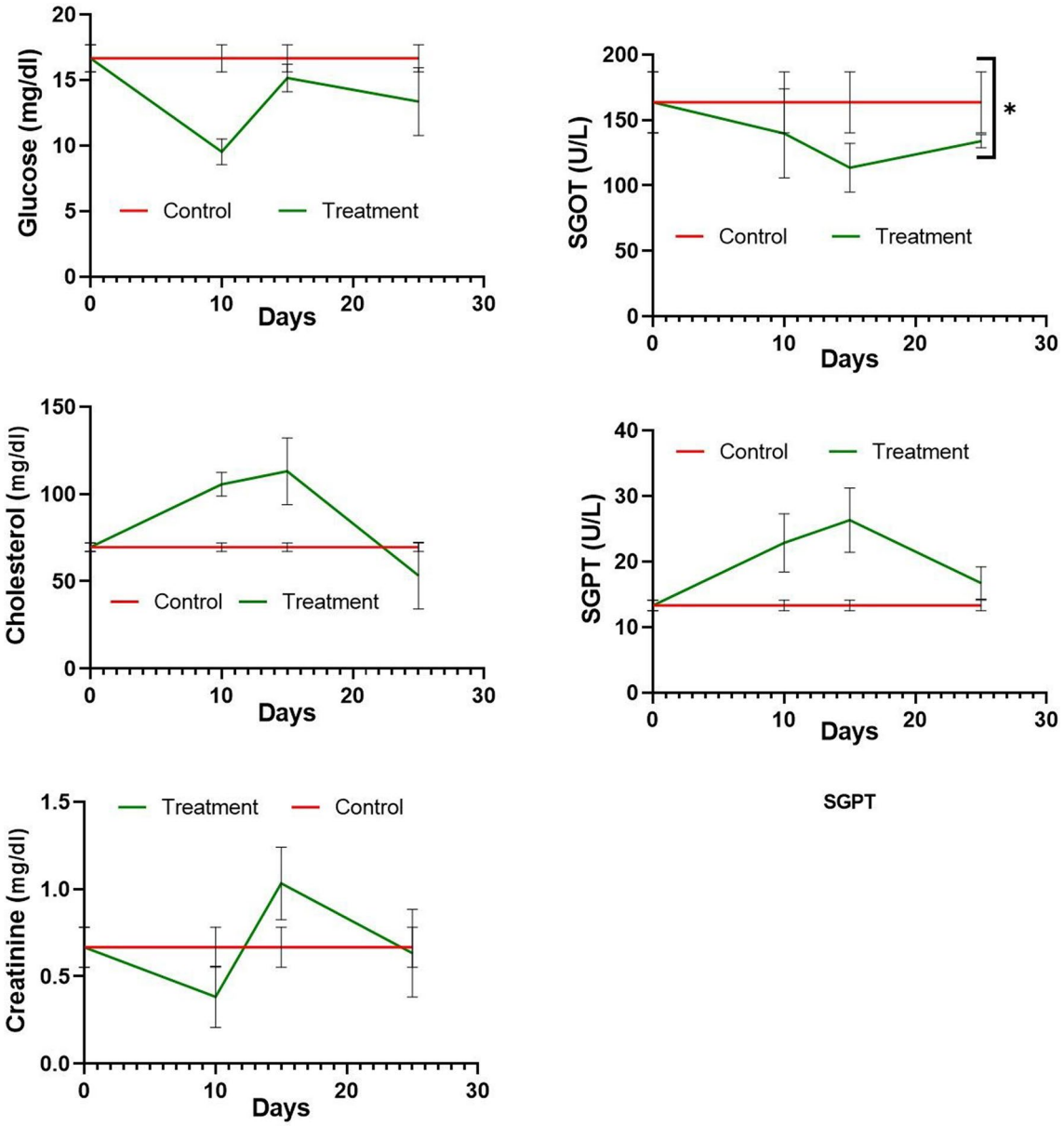

Fig. 5 Effect of Rhodium (III) complex *cis*-[$RhLI_2$]I on biochemical parameter of mice. Serum creatinine, glucose, cholesterol, SGOT, SGPT in normal mice were examined on different days after 10 days treatment. These parameters deteriorate to some extent during treatment period, however, they restored towards normal levels followed the treatment. The results are shown as mean ± SEM and the significant values are $p < 0.05$ when compared to the control

Table 3 Effects of rhodium (III) *cis*-[$RhLI_2$]I complex on blood parameters in normal mice on days 10,15 and, 25

Name of experiment	Days	RBC cells/mL	WBC cells/ mL	% of Hb gm/dL
Normal mice	0	$(5.76 \pm 0.44) \times 10^{09}$	$(9.66 \pm 2.18) \times 10^{6}$	9.03 ± 0.08
Treatment (EAC + 200 µg/kg body weight/day)	10	$(5.01 \pm 1.06) \times 10^{09*}$	$(16.33 \pm 0.88) \times 10^{6*}$	9.4 ± 0.208***
	15	$(7.07 \pm 0.20) \times 10^{09*}$	$(15 \pm 0.57) \times 10^{6*}$	11.6 ± 0.702***
	25	$(8.55 \pm 0.64) \times 10^{09*}$	$(13.33 \pm 0.88) \times 10^{6*}$	13.3 ± 0.251***

The results are presented as mean ± SEM. Significant values are indicated by *$P < 0.05$ and ***$P < 0.001$ when compared to the normal and control groups

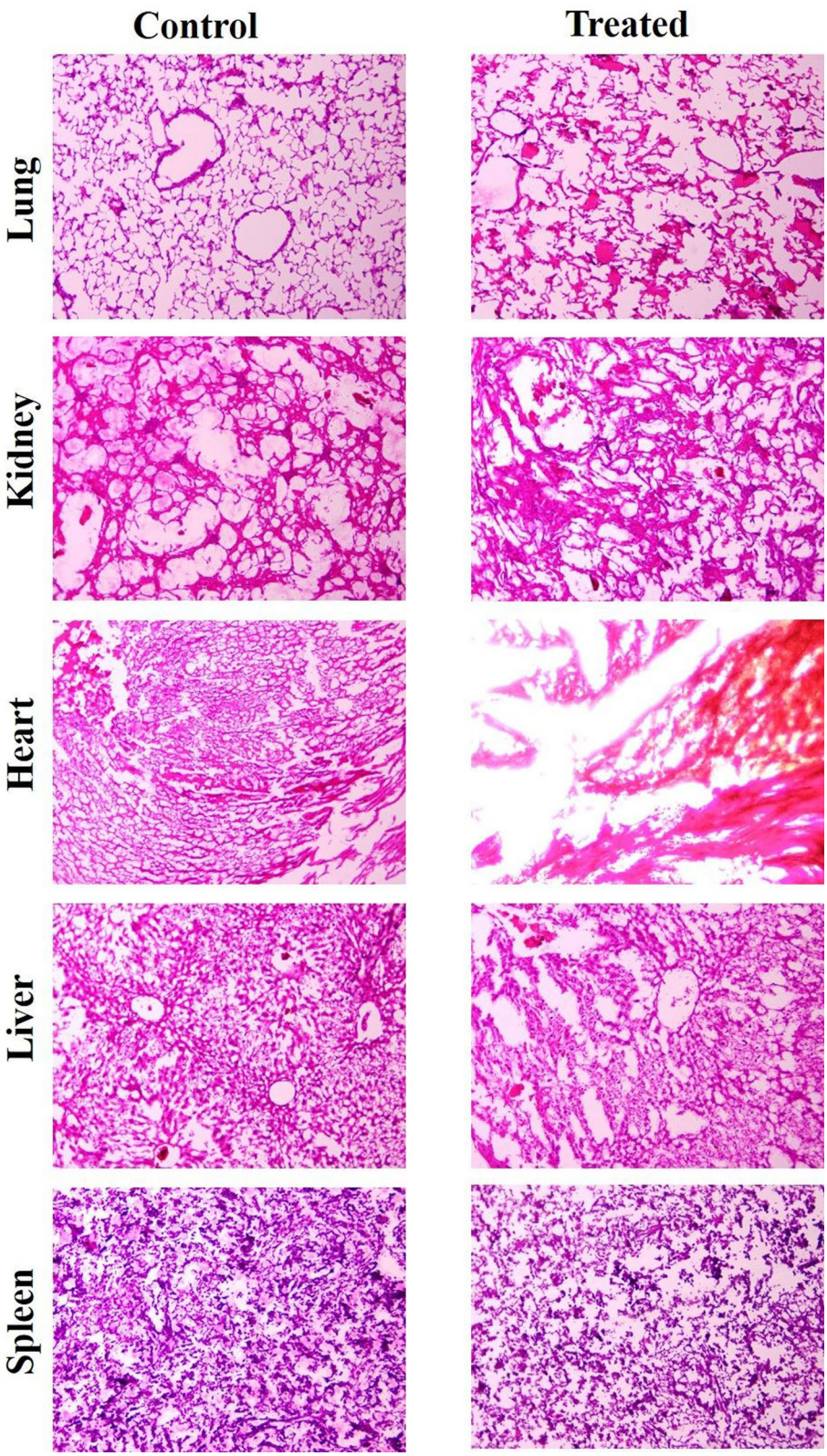

Fig. 6 Effect of Rhodium (III) complex *cis*-[$RhLI_2$] I on tissues of mice. Histopathology of major mice organs mice were examined on day 25 of treatment. There was no alterations or damage noted of the tested mice organs following the treatment

increasing the tumor burden. Consequently, in EAC-bearing mice, anemia manifests through a marked decrease in hemoglobin and RBC levels. Additionally, an elevated WBC count in tumor-bearing mice, indicating an immune response or inflammation linked to tumor progression [39]. Interestingly, we have noted that the treatment with Rhodium complex significantly enhanced the hemoglobin and RBC levels as well as decreased the WBC level in the treatment group

compared to the control. Some studies reported the chemotherapeutic drug-induced anemia by impairing hematopoiesis in cancer patients. Myelosuppression is one of the major drawbacks found in cancer chemotherapy followed by the progression of anemia due to the reduction of RBC and hemoglobin contents in the host [40]. The European Cancer Anemia Survey showed that anemia increased from 19.5% in the first cycle of chemotherapy to 46.7% after the fifth cycle [41]. Another study reported the incidence of anemia was raised to be 90% after treatment with a chemotherapeutic drug [42]. Anemia exerts a negative influence on the quality of life of cancer patients as it may contribute to cancer-induced fatigue [42]. Result from this study noted that treatment with Rhodium complex improved 17.728% Hb level and 18.49141% RBC level back toward the normal level. Thus, we have assumed that it could have a protective effect on the hematopoietic system. Therefore, the potential chemotherapy drug derived from this compound could produce more tolerable drugs with fewer side effects, offering greater protective benefits for cancer patients.

The evasion of apoptosis is an early event in tumor development, enabling abnormal cell proliferation and contributing to cancer progression. Thus, promoting apoptosis in cancer cells while sparing nearby healthy cells is a key mechanism of action for an effective and safer anticancer agent [32]. Consequently, we examined the apoptotic efficiency of Rhodium complex along with underlying mechanism of its anticancer potential using human breast (MCF7) cells. Interestingly, we found that the treatment of with the compound triggered apoptosis of MCF7 cells followed by significant cell growth inhibition. The cells treated with tested compound exhibited apoptotic properties including cell membrane blebbing, the formation of apoptotic bodies, chromosomal condensation, and nuclear fragmentation under a fluorescent microscope. Peng, Yan-Bo et al. (2021) also found the similar results, including cytoplasmic shrinkage, membrane blebbing, chromatin condensation, and nuclear fragmentation after treatment with another Rhodium complex against HeLa cells [10]. Hence, we anticipated that the compound led to a dose-dependent reduction of MCF7 cells growth through the apoptotic mechanism.

To further understand apoptotic pathways activation followed by the compound treatment in MCF7 cells, we evaluated the expression of apoptosis regulatory genes includes p53, BAX, BCL-2, CAS-3, CAS-8, CAS-9, and PARP through RT-qPCR. It is commonly known that p53 controls the process of apoptosis and interacts with members of Bcl-2 family, including Bax [43]. Bax interacts with the mitochondrial outer membrane, leading to the activation of the voltage-dependent anion channel (VDAC). This activation facilitates the permeabilization of the outer membrane, resulting in the release of cytochrome c into the cytosol [43]. However, Bcl-2 is an anti-apoptotic protein that plays a key function in regulating apoptosis [43]. The balance between Bax (pro-apoptotic) and Bcl-2 (anti-apoptotic) proteins plays a pivotal role in regulating cell fate decisions. An increased Bax/Bcl-2 ratio typically signals the initiation of apoptosis, whereas a decreased ratio favors the activation of survival mechanisms [44, 45]. In addition, this ratio was regarded as a useful and trustworthy biomarker for assessing the efficacy of various cancer treatments. Moreover, this ratio allows for precise monitoring of chemotherapy and radiation therapy outcomes, as well as resistance to chemotherapy [46]. In this study, an increased Bax/Bcl-2 expression ratio was observed in MCF7 cells. Thus, it is hypothesized that the upregulation of the Bax interact with the mitochondrial membrane in MCF7 cells. The interaction induces the release of cytochrome C from mitochondria and activates caspase 9 via the development of the apoptosome complex. Clay, Hayley B et al.2011 reported that caspase-9 activates executioner caspases including caspase-3. Caspase-3 is a noteworthy factor in apoptotic signaling pathways and activation of caspase-3 is the key event in triggering apoptosis in tumor cells [47]. However, lacking of caspase 3 protein in MCF7 cells indicating that induction and execution of apoptosis of this cell may occurred by other mechanisms [48]. Thus, herein, overexpression of caspase-9 and down regulation of Bcl-2 were observed in groups treated with the compound, indicating that MCF7 cells treated with this rhodium complex activated apoptotic pathway in MCF7 cells (Fig. 7).

Poly (ADP-ribose) polymerase (PARP) is a protein family that participates in a variety of biological activities, including DNA repair, genomic stability, and programmed cell death [49]. In this study, an increased PARP expression ratio was observed compared to control. PARP activation leads to DNA strand breaks, which ultimately results in apoptosis of cell. This result leads us to assume that the synthetic compound could lead breakage of DNA followed by upregulation of p53, Bax, Caspase-3, −9, and Parp while downregulate anti-apoptotic Bcl2, thereby kill MCF7 cells proliferation by activating intrinsic apoptotic pathway (Fig. 7).

Furthermore, we investigated the expression levels of caspase-8 (CASP8), a crucial cysteine protease that orchestrates the extrinsic apoptotic pathway through its interaction with death receptors. CASP8 is subject to autocatalytic cleavage, resulting in the generation of its active form. Once activated, CASP8 translocates into the cytosol where it cleaves and activates downstream effector caspases, thereby propagating the apoptotic signal [50] Additionally, CASP8 cleaves Bid, a pro-apoptotic BH3-only member of the Bcl-2 family. Cleaved Bid subsequently translocates to the mitochondria, where it amplifies apoptotic signaling by initiating the intrinsic pathway, thereby creating a crosstalk between extrinsic

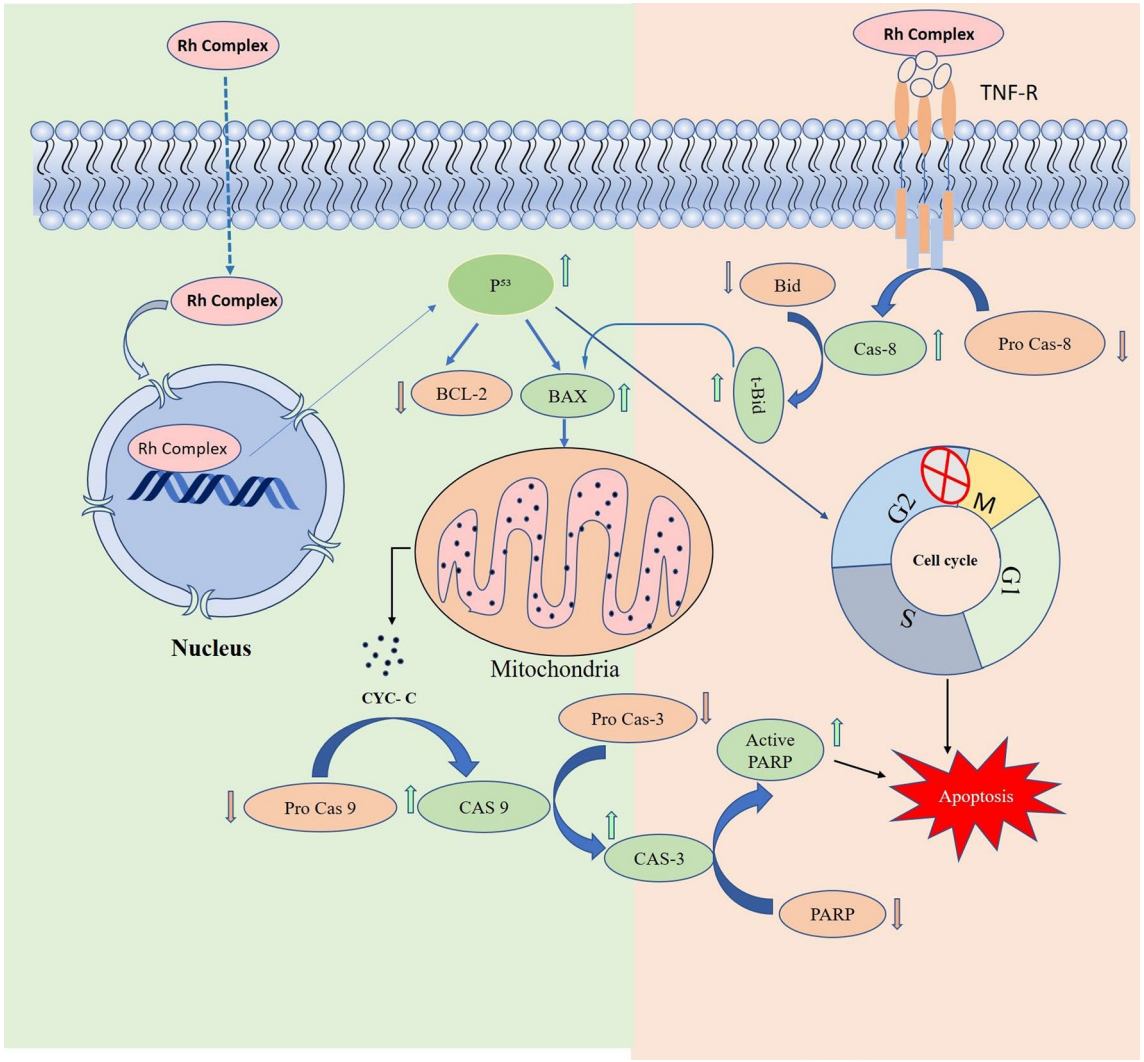

Fig. 7 Possible mechanism of anticancer activity of the compound. Treatment of MCF7 cells with Rhodium (III) complex *cis*-[$RhLI_2$] I induces upregulation od proapoptotic factors such as p53, Bax, Parp, Caspase-3, –8, –9 and downregulates antiapoptotic Bcl2. Upregulation of both caspase-8 and caspase-9 indicating a crosstalk between the extrinsic and intrinsic mitochondrial mechanisms

and intrinsic apoptotic mechanisms (Fig. 7). Interestingly, we have noticed that the treatment with our compound upregulate the cas-8 expression, however, difference did not reach the statistically significant level ($p > 0.05$). Therefore, it could hypothesize that the upregulation of the Cas-8 gene leads to apoptosis in MCF7 cells followed by intrinsic pathway in association with Bid mediated activation of apoptotic signaling.

The assessment of health safety is a critical prerequisite for any compound prior to its development as a therapeutic agent. In addition, chemically synthesized drugs are required to undergo the acute and chronic toxicity studies for further development as a therapeutic lead compound. Accordingly, we have studied the toxicity of the tested compound in mice. Hematological parameters (RBC and Hb) in normal mice treated with the rhodium complex was decreased on day 10 and day 15 due to mild toxicity during treatment period, however, they become normal after completion of treatment (on day 25). On the other hand, WBC was increased moderately during treatment on day 10 and 15, whereas, it regained almost normal value on day 25. Thus, the compound did not have significant adverse effects on the hematological system in mice. Similarly, serum glucose level almost same as normal mice during the treatment period, which was a good sign for health. Also, SGPT and SGOT are important biomarkers of cellular

integrity and function of liver and heart, and are often released into blood from damaged liver [51]. Cellular damage, tissue necrosis and cardiovascular diseases lead to elevation of serum concentrations of these enzymes [52]. We noted that SGOT level slightly changed than normal mice during the treatment period and after treatment they restored towards normal levels, which indicates there was no damage to liver tissue or organs. In addition, SGPT and cholesterol level slightly increased due to mild cardiotoxicity during treatment period, however, they become normal after completion of treatment schedule, which was a good sign for no heart damage or diseases. Creatinine remained the most important markers of renal function and are used in diagnoses of kidney diseases or monitor clinical outcome of a therapy [53]. Creatinine is a byproduct of normal muscle function and it is a metabolite of creatinine phosphate, which the body use as an energy source and elevation of creatinine level is an indication of impaired kidney function because of poor clearance of creatinine in the blood. No significant alteration of serum creatinine level in mice receiving the compound during and after treatment, implied there was no damage to kidney tissue in experimental animals. These results are rectified by the finding of our histopathology of major organs of mice treated with the test compound. There was tissue level damaged was noted in histological tissue sections, which further indicates that the Rhodium complex used in the current study did not have any significant adverse effects on the haematological, biochemical parameters and toxic effects on tissue level. Despite the promising findings, this study has several limitations that may have influenced the breadth and depth of our results. Firstly, limitations in funding restricted access to advanced instrumentation, such as immunoblotting, xenograft models, and high-resolution imaging systems, which could have provided a more detailed analysis of the cancer pathways and molecular mechanisms involved. The absence of these advanced tools limits the ability to conduct comprehensive pathway studies, detect subtle molecular interactions, and validate our findings with high precision. Furthermore, this study was conducted exclusively on the MCF-7 breast cancer cell line, which may limit the generalizability of the results to other cancer types. Testing across multiple cell lines would provide a more robust understanding of the rhodium complex's effects and potential therapeutic applications across a broader spectrum of cancers. Future studies with more extensive funding and access to a range of cell lines and advanced instruments are warranted to expand on these findings and uncover additional insights into cancer apoptosis and treatment response.

In summary, the synthetic Rhodium (III) complex cis-[$RhLI_2$]I exhibited notable anticancer effects in both in vivo and in vitro models. The compound significantly suppressed tumor growth in EAC-bearing Swiss albino mice and triggered apoptosis in MCF-7 cells by upregulating essential apoptosis-related genes, such as p53, Bax, caspase-3, and caspase-9, while downregulating the anti-apoptotic protein Bcl-2. The increase in the Bax/Bcl-2 ratio and the activation of caspases suggest that the Rhodium complex induces apoptosis through the intrinsic mitochondrial pathway. Additionally, the compound enhanced hematological parameters in tumor-bearing mice by restoring hemoglobin and RBC levels and reducing WBC counts, indicating a protective effect on the hematopoietic system. Toxicity assessments showed only mild and transient effects on hematological and biochemical parameters, which returned to normal post-treatment. Notably, no significant damage to the liver, kidney, spleen, lung, or heart tissues was observed during the treatment. Overall, the Rhodium complex appears to be a tolerable chemotherapeutic agent with fewer side effects, offering a promising alternative for cancer chemotherapy development.

Acknowledgements The authors are thankful Indian Institute of Chemical Biology (IICB) Kolkata, India for providing EAC cells.

Author contributions M.M.H., K.S., performed the experiment and drafted the manuscript, M.A.R., A.A., M.T.H.P., K.M. R., analyzed the data and generated figures and tables, M.N., supervised the project, M.H.R., T.G.R., synthesized and characterized the compound, J.A.K., F.I. planned the project and edited the manuscript.

Data availability Data will be made available on request.

Code availability Not applicable.

Declarations

Founding This work was supported by grants from Dean of Science, Rajshahi University, Rajshahi-6205, Bangladesh (Grant No:1019(2)/ 169/BM) and the grants from the Ministry of Science and Technology, Government of People's Republic of Bangladesh (Grant No. NST/2020–21/MSc/MS).

Competing interests The authors state that they have no known competing financial interests or personal relationships that could have influenced the work reported in this study.

References

1. Liu Y, Zheng Z. Understanding the global cancer statistics 2022: growing cancer burden. Sci China Life Sci. 2024;67(10):2274–6.
2. Siegel RL, Giaquinto NA, Jemal A. Cancer statistics. CA Cancer J Clin. 2024. https://doi.org/10.3322/caac.21820.
3. Badheeb AM, et al. Anemia profiles in cancer patients: prevalence, contributing factors, and insights from a retrospective study at a single cancer center in Saudi Arabia. Cureus. 2023. https://doi.org/10.7759/cureus.42400.
4. Ferlay J, et al. Estimates of worldwide burden of cancer in 2008: GLOBOCAN 2008. Int J Cancer. 2010;127(12):2893–917.
5. Alghamdi AH, et al. Prevalence of anemia among gynecologic cancer patients who received chemotherapy, radiotherapy, or a combination of both at King Abdulaziz medical city, Jeddah. Cureus. 2021. https://doi.org/10.7759/cureus.17613.
6. Cragg GM, Pezzuto JM. Natural products as a vital source for the discovery of cancer chemotherapeutic and chemopreventive agents. Med Princ Pract. 2016;25(Suppl. 2):41–59.
7. Sohrabi M, et al. Recent advances in biological activities of rhodium complexes: their applications in drug discovery research. Eur J Med Chem. 2021;216:113308.
8. Gras M, et al. Anticancer activity of new organo-ruthenium, rhodium and iridium complexes containing the 2-(pyridine-2-yl) thiazole N, N- chelating ligand. J Organomet Chem. 2010;695(8):1119–25.
9. Threatt SD, et al. In vivo anticancer activity of a rhodium metalloinsertor in the HCT116 xenograft tumor model. Proc Natl Acad Sci. 2020;117(30):17535–42.
10. Peng YB, et al. Mitochondria-targeted cyclometalated rhodium (III) complexes: synthesis, characterization and anticancer research. Dalton Trans. 2021;50(26):9068–75.
11. Guo Y, et al. P-glycoprotein (P-gp)-driven cancer drug resistance: biological profile, non-coding RNAs, drugs and nanomodulators. Drug Discov Today. 2024;29:104161.
12. Qin Y, et al. Autophagy and cancer drug resistance in dialogue: pre-clinical and clinical evidence. Cancer lett. 2023;570:216307.
13. Zhou L, et al. HULC targets the IGF1R–PI3K-AKT axis in trans to promote breast cancer metastasis and cisplatin resistance. Cancer Lett. 2022;548:215861.
14. Zheng W, et al. Multi-targeted anticancer agents. Cur Top Med Chem. 2017;17(28):3084–98.
15. Leung CH, et al. Bioactive iridium and rhodium complexes as therapeutic agents. Coord Chem Rev. 2013;257(11–12):1764–76.
16. Sudding LC, et al. Evaluation of the in vitro anticancer activity of cyclometalated half-sandwich rhodium and iridium complexes coordinated to naphthaldimine-based poly (propyleneimine) dendritic scaffolds. J Organomet Chem. 2014;774:79–85.
17. Máliková K, Masaryk L, Štarha P. Anticancer half-sandwich rhodium (III) complexes. Inorganics. 2021;9(4):26.
18. Yang GJ, et al. Selective inhibition of lysine-specific demethylase 5A (KDM5A) using a rhodium (III) complex for triple-negative breast cancer therapy. Angew Chem. 2018;130(40):13275–9.
19. Ma DL, et al. Antagonizing STAT3 dimerization with a rhodium (III) complex. Angew Chem. 2014;126(35):9332–6.
20. Gasser G, Metzler-Nolte N. The potential of organometallic complexes in medicinal chemistry. Curr Opin Chem Biol. 2012;16(1–2):84–91.
21. Khan TM, et al. Rhodium (III) complexes with isoquinoline derivatives as potential anticancer agents: in vitro and in vivo activity studies. Dalton Trans. 2019;48(30):11469–79.
22. Markham J, et al. (Pentamethylcyclopentadienato) rhodium complexes for delivery of the curcumin anticancer drug. Eur J Inorg Chem. 2017;2017(12):1812–23.
23. Petrović A, et al. Synthesis of camphor-derived bis (pyrazolylpyridine) rhodium (III) complexes: structure–reactivity relationships and biological activity. Inorg Chem. 2018;58(1):307–19.
24. Hartinger CG, Dyson PJ. Bioorganometallic chemistry—from teaching paradigms to medicinal applications. Chem Soc Rev. 2009;38(2):391–401.
25. Bembi R, et al. Polyazamacrocycles. V. structure of isomeric 3, 5, 7, 7, 10, 12, 14, 14-octamethyl-1, 4, 8, 11-tetraazacyclotetradecanes. Bull Chem Soc Jpn. 1989;62(11):3701–5.
26. Rabi S, Paul P, Hazari SKS, Dey BK, Palit D, Rahman IMM, Roy TG. Rhodium(III) and platinum(II) complexes of azamacrocycle: synthesis, characterization and antimicrobial evaluation. Asian J Chem. 2022;34(9):2444–50.
27. Khanam JA, et al. Antineoplastic activity of acetone semicarbazone (ASC) against Ehrlich ascites carcinoma (EAC) bearing mice. J Natl Sc Found Sri Lanka. 2010. https://doi.org/10.4038/jnsfsr.v38i4.2649.
28. Islam F, et al. A p-Menth-1-ene-4, 7-diol (EC-1) from *Eucalyptus camaldulensis Dhnh*. Triggers apoptosis and cell cycle changes in ehrlich ascites carcinoma cells. Phytother Res. 2015;29(4):573–81.
29. Yesmin R, et al. Anticancer potential of *Michelia champaca Linn*. bark against Ehrlich ascites carcinoma (EAC) cells in Swiss albino mice. Nat Prod J. 2021;11(1):85–96.
30. Perveen R, et al. Preventive effect of ethanol extract of *Alpinia calcarata Rosc* on Ehrlich's ascitic carcinoma cell induced malignant ascites in mice. Asian Pac J Trop Med. 2012;5(2):121–5.
31. Nurujjaman M, et al. Antitumor activity of a lectin purified from *Punica granatum Pulps* against Ehrlich Ascites Carcinoma (EAC) cells. Anti Cancer Agents Med Chem. 2024;24(3):193–202.

32. Siddika A, et al. Antiproliferative activity and apoptotic efficiency of *Syzygium cumini* bark methanolic extract against EAC cells in vivo. Anti Cancer Agents Med Chem. 2021;21(6):782–92.
33. Khatun M, et al. 2′, 4′-dihydroxy-3, 4-methylenedioxychalcone activate mitochondrial apoptosis of Ehrlich Ascites carcinoma cells. Curr Drug Ther. 2020;15(4):337–50.
34. Islam F, Ghosh S, Khanam JA. Antiproliferative and hepatoprotective activity of metabolites from *Corynebacterium xerosis* against Ehrlich ascites carcinoma cells. Asian Pac J Trop Biomed. 2014;4:S284–92.
35. Islam F, Ali SMM, Khanam JAra. Hepatoprotective effect of acetone semicarbazone on Ehrlich ascites carcinoma induced carcinogenesis in experimental mice. Asian Pac J Trop Biomed. 2013;3(2):105–10.
36. Ghareeb MA, et al. Antioxidant and cytotoxic activities of *Tectona grandis Linn* leaves. Int J Phytopharmacol. 2014;5(2):143–57.
37. Roy MR, Guhathakurta S, Roychowdhury J. Hematological changes in experimental tumors. Indian J Med Res. 1981;74:896–903.
38. Adamson JW. The anemia of inflammation/malignancy: mechanisms and management. ASH Educ Progr B. 2008;2008(1):159–65.
39. Wang C, et al. Low local blood perfusion, high white blood cell and high platelet count are associated with primary tumor growth and lung metastasis in a 4T1 mouse breast cancer metastasis model. Oncol Lett. 2015;10(2):754–60.
40. Aravind SR, et al. Antitumor and immunopotentiating activity of polysaccharide PST001 isolated from the seed kernel of *Tamarindus indica*: an in vivo study in mice. Sci World J. 2012;2012(1): 361382.
41. Ludwig H, et al. The European cancer anaemia survey (ECAS): a large, multinational, prospective survey defining the prevalence, incidence, and treatment of anaemia in cancer patients. EurJ Cancer. 2004;40(15):2293–306.
42. Dicato M, Plawny L, Diederich M. Anemia in cancer. Ann Oncol. 2010. https://doi.org/10.1093/annonc/mdq284.
43. Shendge AK, et al. A natural flavonoid, apigenin isolated from *Clerodendrum viscosum* leaves, induces G2/M phase cell cycle arrest and apoptosis in MCF-7 cells through the regulation of p53 and caspase-cascade pathway. Clin Transl Oncol. 2021;23:718–30.
44. Perlman H, et al. An elevated bax/bcl-2 ratio corresponds with the onset of prostate epithelial cell apoptosis. Cell Death Diff. 1999;6(1):48–54.
45. Ghate NB, et al. Sundew plant, a potential source of anti-inflammatory agents, selectively induces G2/M arrest and apoptosis in MCF-7 cells through upregulation of p53 and Bax/Bcl-2 ratio. Cell Death Discov. 2016;2(1):1–10.
46. Khodapasand E, et al. Is Bax/Bcl-2 ratio considered as a prognostic marker with age and tumor location in colorectal cancer? Iran Biomed J. 2015;19(2):69.
47. Clay HB, Sillivan S, Konradi C. Mitochondrial dysfunction and pathology in bipolar disorder and schizophrenia. Int J Dev Neurosci. 2011;29(3):311–24.
48. Jänicke RU. MCF-7 breast carcinoma cells do not express caspase-3. Breast Cancer Res Treat. 2009;117(1):219–21.
49. Herceg Z, Wang ZQ. Functions of poly (ADP-ribose) polymerase (PARP) in DNA repair, genomic integrity and cell death. Mutat Res Fundam Mol Mech Mutagen. 2001;477(1–2):97–110.
50. Kominami K, et al. The molecular mechanism of apoptosis upon caspase-8 activation: quantitative experimental validation of a mathematical model. Biochim Et Biophys Acta BBA Mol Cell Res. 2012;1823(10):1825–40.
51. Chavda R, Vadalia KR, Gokani RL. Hepatoprotective and antioxidant activity of root bark of *Calotropis procera* R. Br (asclepediaceae). Int J Pharmacol. 2010. https://doi.org/10.3923/ijp.2010.937.943.
52. Adeyemi OT, et al. Alkaline phosphatase (ALP), aspartate aminotransferase (AST) and alanine aminotransferase (ALT) activities in selected tissues of rats fed on processed Atlantic horse mackerel (Trachurus trachurus). Adv Biosci Biotechnol. 2015;6(03):139–52.
53. Alomar MY. Physiological and histopathological study on the influence of *Ocimum basilicum* leaves extract on thioacetamide-induced nephrotoxicity in male rats. Saudi J Boil Sci. 2020;27(7):1843–9.